Crystal Structure and Site Preference of Ba-Doped α-Tricalcium Phosphate $(Ca_{1-x}Ba_x)_3(PO_4)_2$ through High-Resolution Synchrotron Powder Diffraction ($x = 0.05$ to 0.15)

Masatomo Yashima* and Yoichi Kawaike

Department of Materials Science and Engineering, Interdisciplinary Graduate School of Science and Engineering, Tokyo Institute of Technology, Nagatsuta-cho 4259, Midori-ku, Yokohama-shi, Kanagawa 226-8502, Japan

Received April 6, 2007. Revised Manuscript Received May 27, 2007

The single phase of barium-substituted alpha tricalcium phosphate (Ba-α-TCP) $(Ca_{1-x}Ba_x)_3(PO_4)_2$ ($x = 0.05$, 0.10, and 0.15) has been prepared by solid-state reactions. The crystal structure of the Ba-α-TCP powders has been investigated by high-resolution synchrotron powder diffraction and the Rietveld method. Diffraction data were successfully analyzed by the single phase Ba-α-TCP (space group $P2_1/a$). Unit-cell parameters a, b, c, and β increase with increasing Ba content. Most of the Ba atoms are located at three crystallographic sites among the eighteen cation sites in the α-$(Ca_{1-x}Ba_x)_3(PO_4)_2$ ($x = 0.05$, 0.10, and 0.15). The refined positional parameters and occupancy factors of the preference sites for Ba substitutions were Ca17: (0.0909(6), 0.4167(2), 0.7823(5)) g(Ba) = 0.72(2); Ca11: (0.4068(6), 0.2506(2), 0.2199(5)) g(Ba) = 0.67(1); Ca5: (0.0983(6), 0.0837(2), 0.7857(5)) g(Ba) = 0.65(1) in the α-$(Ca_{0.85}Ba_{0.15})_3(PO_4)_2$. Here, g(Ba) is the occupancy factor of Ba atoms. These sites have relatively smaller bond valence sums, indicating the preference sites for the larger-sized Ba substitutions.

Introduction

Calcium phosphates (CP) and CP-containing materials have been studied extensively for bone substitute applications because the composition of the inorganic component of bone is similar to calcium-deficient carbonated apatite.[1−5] Biomaterials with suitable composition and porosity are resorbed in the body, releasing phosphates and calcium ions that are used by the organism for regenerating natural bone. Bone material is conducive to trace metal substitutions in both cation and anion sites, including Na, Mg, Sr, Al, B, Cd, Pb, Cr, and Si.[1] Many researchers have investigated the effect of doping on the structural, physical, and chemical properties of apatite materials.[1,5]

Tricalcium phosphate [TCP: $Ca_3(PO_4)_2$] is one of the most important biomaterials for bone substitute applications as well as apatites.[1,6,7,8] TCP has at least three polymorphs, i.e., the β-, α-, and α′-phases, depending on the temperature.[1] The β-TCP with a rhombohedral structure (space group $R3c$)[9,10] is stable up to 1125 °C.[11] The monoclinic α-TCP, which has a complicated crystal structure with the space group $P2_1/a$[12−14] is stable between 1125 °C and 1430 °C and can be maintained down to room temperature as a metastable phase. The α′-TCP is stable above 1430 °C and unable to survive quenching to room temperature.[11,13] Recently, the β' phase has also been reported between the low-temperature β and high-temperature α phase.[15] The solubility of α-TCP is about ten times higher than that of hydroxyapatite.[8]

Unit-cell parameters and crystal structure of nondoped and doped β-TCP has extensively been studied by numerous researchers.[9,15−22] Far less attention has been devoted to

* Author to whom correspondence should be addressed. E-mail: yashima@materia.titech.ac.jp.

(1) Elliott, J. C. *Structure and chemistry of the apatites and other calcium orthophosphates*; Elsevier: Amsterdam, 1994.
(2) Suchanek, W.; Yoshimura, M. *J. Mater. Res.* **1998**, *13* (1), 94−116.
(3) Boher, M. *Injury* **2000**, *31* (4), 37−47.
(4) Kotobuki, N.; Ioku, K.; Kawagoe, D.; Fujimori, H.; Goto, S.; Ohgushi, H. *Biomaterials* **2005**, *26* (7), 779−785.
(5) Leventouri, Th.; Bunaciu, C. E.; Perdikatsis, V. *Biomaterials* **2003**, *24* (23), 4205−4211.
(6) Bigi, A.; Compostella, L.; Fichera, A. M.; Foresti, E.; Gazzano, M.; Ripamonti, A.; Roveri, N. *J. Inorg. Biochem.* **1988**, *34* (2), 75−82.
(7) Young, R. A.; Brown, W. E. Structures of biological minerals. In *Biological Mineralization and Demineralization*; G. W. Nancollas, Ed.; Springer-Verlag: Berlin, 1982; pp 101−141.
(8) Makishima, A.; Aoki, H. In *Bioceramics*; Yamagushi, T.; Yanagida, H., Eds.; Giho-do Pub. Co.: Tokyo 1984; p 28.
(9) Yashima, M.; Sakai, A.; Kamiyama, T.; Hoshikawa, A. *J. Solid State Chem.* **2003**, *175*, 272−277.
(10) Dickens, B.; Schroeder, L. W.; Brown, W. E. *J. Solid State Chem.* **1974**, *10* (3), 232−247.
(11) Welch, J. H.; Gutt, W. J. *J. Chem. Soc.* **1961**, *1961*, 4442−4444.
(12) Mathew, M.; Schroeder, L. W.; Dickens, B.; Brown, W. E. *Acta Crystallogr. B* **1977**, *33*, 1325−1333.
(13) Yashima, M.; Sakai, A. *Chem. Phys. Lett.* **2003**, *372* (5−6), 779−783.
(14) Yashima, M.; Kawaike, Y.; Tanaka, M. *J. Am. Ceram. Soc.* **2007**, *90* (1), 272−274.
(15) Belik, A. A.; Izumi, F.; Stefanovich, S. Y.; Malakho, A. P.; Lazoryak, B. I.; Leonidov, I. A.; Leonidova, O. N.; Davydov, S. A. *Chem. Mater.* **2002**, *14* (7), 3197−3205.
(16) Le Geros, R. Z. *J. Dent. Res.* **1974**, *53*, 45−50.
(17) Schroeder, L. W.; Dickens, B.; Brown, W. E. *J. Solid State Chem.* **1977**, *22*, 253−262.
(18) Obadia, L.; Deniard, P.; Alonso, B.; Rouillon, T.; Jobic, S.; Guicheux, J.; Julien, M.; Massiot, D.; Bujoli, B.; Bouler, J. M. *Chem. Mater.* **2006**, *18* (6), 1425−1433.
(19) Enderle, R.; Götz-Neunhoeffer, F.; Göbbels, M.; Müller, F. A.; Greil, P. *Biomaterials* **2005**, *26* (17), 3379−3384.
(20) Wei, X.; Akinc, M. *Key Eng. Mater.* **2005**, *284−286*, 83−86.
(21) Bigi, A.; Foresti, E.; Gandolfi, M.; Gazzano, M.; Roveri, N. *J. Inorg. Biochem.* **1997**, *66* (4), 259−265.
(22) Bigi, A.; Falini, G.; Foresti, E.; Ripamonti, A.; Gazzano, M.; Roveri, N. *Z. Kristallogr.* **1996**, *211* (1), 13−16.

10.1021/cm070963y CCC: $37.00
Published on Web 07/17/2007

nondoped and doped α-TCP. This is partly attributable to the complex crystal structure of α-TCP. The α-TCP has a large unit cell: $a = 12.87271(9)$, $b = 27.28034(8)$, $c = 15.21275(12)$ Å, $\alpha = \gamma = 90°$ and $\beta = 126.2078(4)°$.[14] There exist 18 independent calcium sites, 48 oxygen sites, and 12 phosphor sites in a unit cell of the α-TCP,[12] yielding a complex powder diffraction pattern.[14] Reid et al.[23,24] prepared Si-substituted α-TCP materials and examined their unit-cell parameters as a function of Si composition through a laboratory-based X-ray powder diffractometer. In the Si-substituted samples, the α-TCP, β-TCP, and hydroxyapatite phases coexisted, and the phase composition varied with the silicon content. Furthermore, the laboratory-based X-ray powder diffraction instrument has lower angular resolution even if the Cu *K*α X-ray with relatively long wavelength is used.[14] Thus, it is difficult to obtain detailed crystallographic information on α-TCP.

Since most α-TCP materials are powders or polycrystalline materials, it is important to obtain detailed crystallographic information from powder diffraction patterns of α-TCP. To differentiate as many of the reflection peaks in the powder diffraction profile from one another as possible, we have used high-resolution powder diffractometers and succeeded in determining the precise unit-cell parameters of undoped α-TCP[14] and other materials.[25−27] In the present study, we focus on the unit-cell parameters and crystal structure of Ba-substituted α-TCP. Barium was chosen as dopant because the ionic radius of Ba is large, and we can expect considerable changes in the unit-cell parameters. Ba-doping decreases the transition temperature of the $\beta-\alpha$ transformation and stabilizes the high-temperature metastable α-TCP to room temperature.[28] Thus, we can expect the phase composition of α-TCP to be higher, enabling precise structural analysis.

The purpose of the present study is to investigate the unit-cell parameters and site occupancy of Ba-substituted α-TCP, $(Ca_{1-x}Ba_x)_3(PO_4)_2$ ($x = 0.05$, 0.10, and 0.15), through a high-resolution synchrotron powder diffractometer.

Experiments and Data Processing

Sample Preparation. High-purity Ba-substituted α-TCP, i.e., $(Ca_{1-x}Ba_x)_3(PO_4)_2$ samples ($x = 0.05$, 0.10, and 0.15), were prepared by solid-state reactions using β-TCP (β-$Ca_3(PO_4)_2$) and $Ba_3(PO_4)_2$. Figure 1 shows the synthesis procedure for Ba-α-TCP.

The β-TCP was prepared by solid-state reactions from $CaHPO_4$ and $CaCO_3$.[9,14] Stoichiometric amounts of high-purity $CaHPO_4$ (99.6% purity, Kyowa Chemical Industry Co., Ltd., Takamatsu, Japan) and $CaCO_3$ (99.99% purity, Kojundo Chemical Lab. Co., Ltd., Sakado, Japan) powders were mixed for about 3 h in an agate mortar. The mixture was pressed into pellets under a uniaxial pressure of 150 MPa. The pellets were sintered for 12 h at 1000 °C to obtain the β-TCP. The sintered material was crushed and ground into powders for X-ray diffraction measurements. The resultant product was confirmed to be a single phase of β-TCP using a Rint-2550V/PC laboratory-based X-ray powder diffractometer at room temperature (Figure 2(a)).

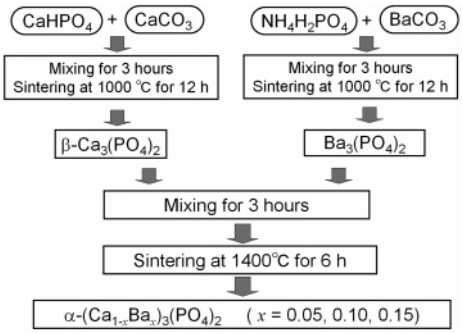

Figure 1. Flow chart for the synthesis of α-$(Ca_{1-x}Ba_x)_3(PO_4)_2$ ($x = 0.05$, 0.10, 0.15).

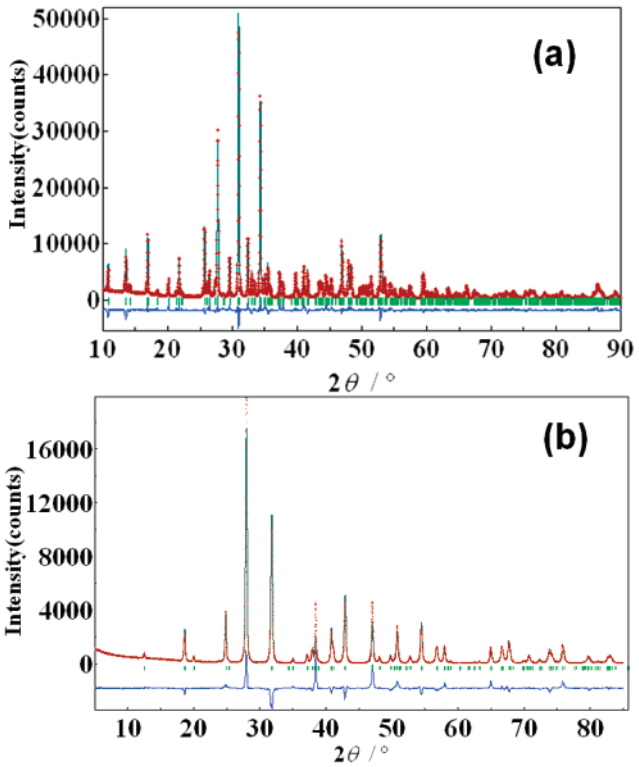

Figure 2. Rietveld analysis patterns for laboratory-based Cu *K*α X-ray powder diffraction data of (a) β-TCP (β-$Ca_3(PO_4)_2$) and of (b) $Ba_3(PO_4)_2$ sample. The solid lines are calculated intensities, and the crosses are the observed intensities. The short vertical lines show the position of Bragg reflections of the calculated pattern. The difference between the observed and calculated intensities is plotted below the profiles.

Stoichiometric amounts of high-purity $NH_4H_2PO_4$ (>99% purity, Kanto Chemical Co., Ltd., Tokyo, Japan) and $BaCO_3$ (>99.9% purity, Kanto Chemical Co., Ltd., Tokyo, Japan) powders were mixed in an agate mortar. The mixture was pressed into pellets under a uniaxial pressure of 150 MPa. The pellets were sintered for 12 h at 1000 °C to obtain the $Ba_3(PO_4)_2$. The sintered material was crushed and ground into powders for X-ray diffraction measurements. The resultant product was confirmed to be the $Ba_3(PO_4)_2$ using the Rint-2550V/PC X-ray powder diffractometer at room temperature (Figure 2(b)).

The β-TCP and $Ba_3(PO_4)_2$ powders were mixed for about 3 h in an agate mortar and pressed into pellets under a uniaxial pressure of 150 MPa. The pellets were sintered for 6 h at 1400 °C to obtain a single phase of α-$(Ca_{1-x}Ba_x)_3(PO_4)_2$ ($x = 0.05$, 0.10, and 0.15).

(23) Reid, J. W.; Pietak, A.; Sayer, M.; Dunfield, D.; Smith, T. J. N. *Biomaterials* **2005**, *26* (16), 2887−2897.
(24) Reid, J. W.; Tuck, L.; Sayer, M.; Fargo, K.; Hendry, J. A.; *Biomaterials* **2006**, *27* (15), 2916−2925.
(25) Yashima, M. *J. Am. Ceram. Soc.* **2002**, *85* (12), 2925−2930.
(26) Yashima, M.; Mori, M.; Ali, R.; Tanaka, M.; Mori, T. *Chem. Phys. Lett.* **2003**, *371* (5−6), 582−587.
(27) Yashima, M.; Tsunekawa, S. *Acta Crystallogr. B* **2006**, *62* (1), 161−164.
(28) Keridler, E. R. *J. Electrochem. Soc.* **1972**, *118* (6), 923−929.

Table 1. Chemical Compositions, Reliability Factors, and Refined Unit-Cell Parameters of Ba-Substituted α-TCP, $(Ca_{1-x}Ba_x)_3(PO_4)_2$. Chemical Analysis Results $[(Ca_{1-x}Ba_x)_y(PO_4)_2]$ for the Ba-α-TCP (space group $P2_1/a$)[a]

	composition x		
	0.05	0.10	0.15
	Chemical Analysis Results		
x	0.052(8)	0.101(1)	0.152(6)
y	3.00(2)	3.05(3)	2.99(13)
	Reliability Factors		
R_{wp} (%)	8.17	7.20	5.41
R_p (%)	6.27	5.59	4.13
S	1.85	1.72	1.94
R_I (%)	5.09	3.59	2.74
R_F (%)	3.95	2.76	1.84
	Unit Cell Parameters		
a (Å)	12.95927(18)	13.0326(2)	13.0965(2)
b (Å)	27.58125(19)	27.7430(2)	27.9046(3)
c (Å)	15.2552(2)	15.3141(2)	15.4021(3)
$\alpha = \gamma$ (deg)	90	90	90
β (deg)	126.6688(7)	126.8963(10)	127.1224(9)
V (Å^3)	4373.62(8)	4428.12(12)	4488.06(12)

[a] All the structural parameters are described in CIF files of the Supporting Information.

The sintered material was crushed and ground into powders for X-ray diffraction measurements. The resultant product was confirmed to be α-$(Ca_{1-x}Ba_x)_3(PO_4)_2$ using the X-ray powder diffractometer at room temperature.

Chemical compositions x and y in the resultant products $(Ca_{1-x}Ba_x)_y(PO_4)_2$ were determined by chemical analysis. The results indicated that the Ba/Ca atomic ratio agreed well with the nominal composition and that the cation/P atomic ratio was stoichiometric $y = 3.00$ (Table 1).

Synchrotron Powder Diffraction Experiments and Data Processing. Synchrotron X-ray powder diffraction experiments on the α-$(Ca_{1-x}Ba_x)_3(PO_4)_2$ samples ($x = 0.05$, 0.10, and 0.15) were performed using the multiple-detector system[29] installed at the BL-4B$_2$ beam line of the Photon Factory, High Energy Accelerator Research Organization (KEK), Japan. The experimental setup consisted of a bending-magnet light source, a double-crystal Si-(111) monochromator, a focusing cylindrical mirror, and a multiple-detector system with Ge(111) analyzer crystals, Soller slits, and scintillation counters.[29] A monochromatized 1.20628(4) Å X-ray beam was utilized. Powder diffraction data from the sample at 298 K in air were collected in asymmetric flat-specimen reflection geometry with a fixed incident angle of 7.0°. Scanning parameters were set as follows: step interval: 0.008°; counting time: 3 s step^{-1}; diffraction angle (2θ): 8−80°. The crystal structures of the α-$(Ca_{1-x}Ba_x)_3(PO_4)_2$ samples were refined by the Rietveld method using RIETAN-2000.[30] As enhancement in the asymmetric scan mode is not implemented in RIETAN-2000, the observed intensity data were modified by multiplying by the term $[1 + \{\sin\alpha/\sin(2\theta - \alpha)\}]/2$, where α is the fixed incident angle, in order to obtain data equivalent to those measured in the symmetric scan mode.[31] The peak shape was assumed to be a modified split pseudo-Voigt function.[29] The cutoff value was set at 7.00 × fwhm. The background was approximated by a 12-variable polynomial in $2\theta^n$ ($n = 0...11$). Twelve parameters in the polynomial were refined simultaneously with the unit cell, zero point, scale, profile shape, and crystal structural parameters.

(29) Toraya, H., Hibino, H., Ohsumi, K. *J. Synchr. Rad.* **1996**, *3* (2), 75−83.
(30) Izumi, F.; Ikeda, T. *Mater. Sci. Forum* **2000**, *321−324*, 198−204.
(31) Toraya, H.; Huang, T. C.; Wu, Y. *J. Appl. Crystallogr.* **1993**, *26* (pt 6), 774−777.

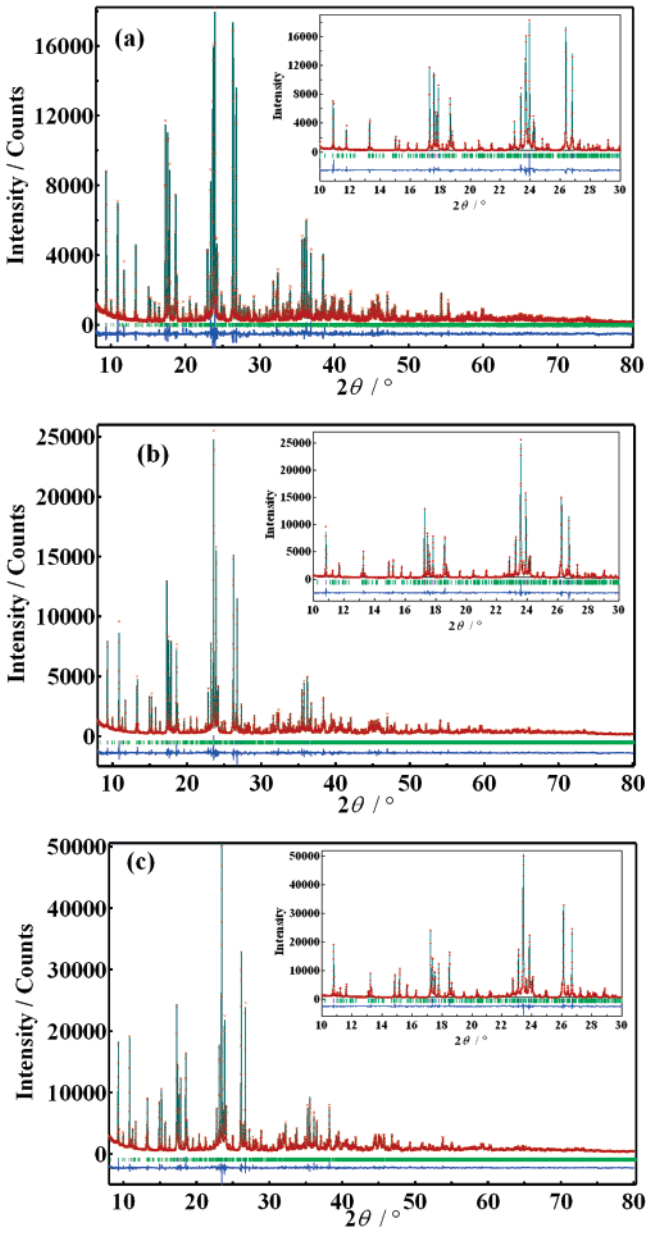

Figure 3. Rietveld analysis patterns for synchrotron powder diffraction data of Ba-substituted α-TCP, $(Ca_{1-x}Ba_x)_3(PO_4)_2$ samples ((a) $x = 0.05$, (b) $x = 0.10$, and (c) $x = 0.15$). Insets are enlarged patterns. The solid lines are the calculated intensities, and the crosses are the observed intensities. The short vertical lines show the position of Bragg reflections of the calculated pattern. The difference between the observed and calculated intensities is plotted below the profiles. A monochromatized 1.20628(4) Å X-ray beam was utilized.

Results and Discussion

Figure 3 shows the Rietveld patterns of the synchrotron powder diffraction profile of the Ba-substituted α-TCP, i.e., $(Ca_{1-x}Ba_x)_3(PO_4)_2$ samples ((a) $x = 0.05$, (b) $x = 0.10$, and (c) $x = 0.15$). No stable β-TCP was found in the present specimens owing to either the sluggish kinetics of the α-to-β transformation or stabilizing of α phase by the Ba doping. Structural refinement of the α-TCP was performed by a monoclinic structure, namely, space group $P2_1/a$. The structural parameters reported in the literature[12,14] were used as initial parameters in the Rietveld analysis. The calculated intensity agreed well with the observed data (Figure 3). The refined unit-cell parameters and reliability factors are listed

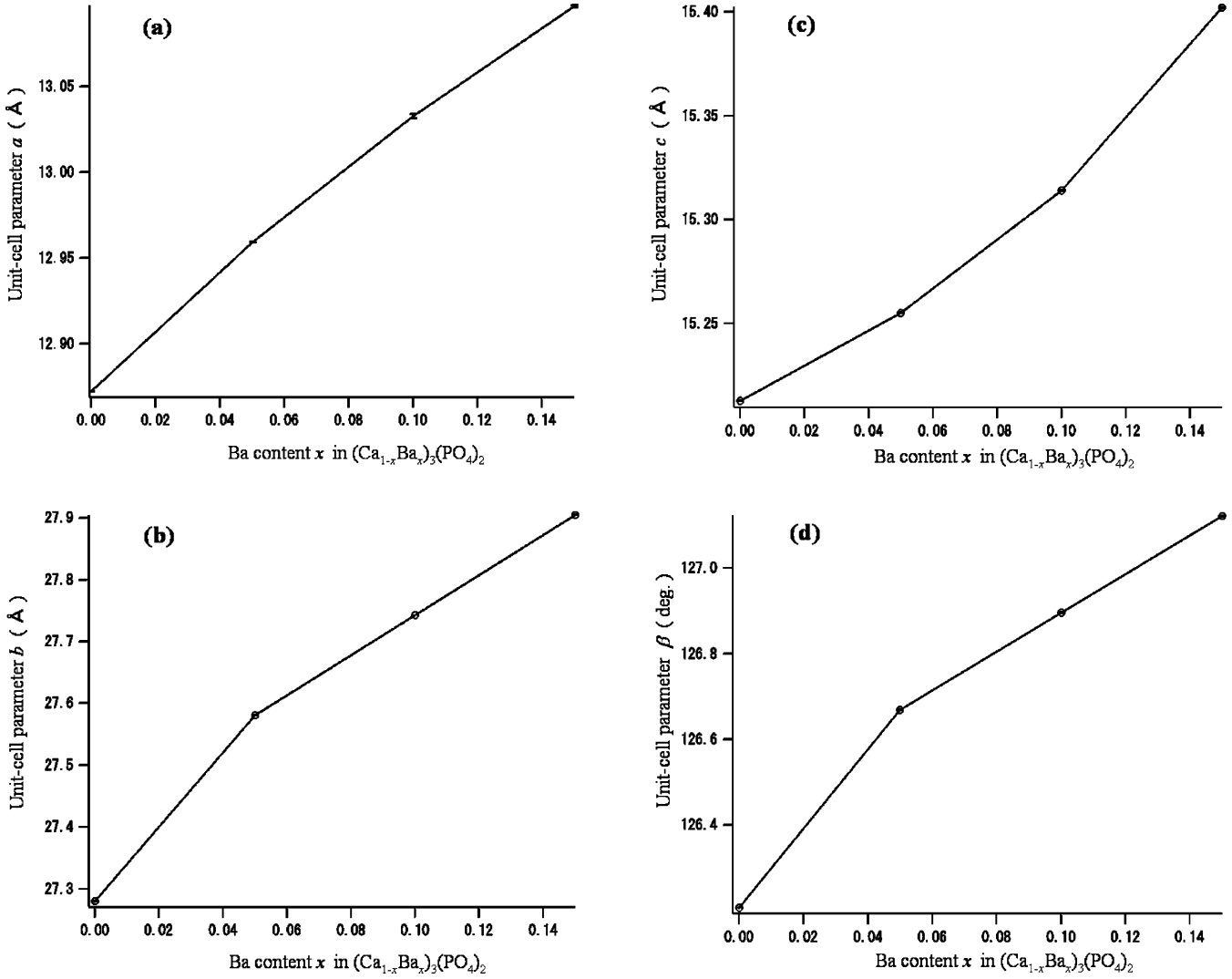

Figure 4. Unit-cell parameters of the Ba-substituted α-TCP as functions of Ba content x in $(Ca_{1-x}Ba_x)_3(PO_4)_2$. Data for $x = 0$ is taken from our previous high-resolution synchrotron diffraction work.[14] Error bars of standard uncertainties in the Rietveld analysis are smaller than the datum symbols.

in Table 1. For example, for the $(Ca_{0.85}Ba_{0.15})_3(PO_4)_2$ composition, the reliability factors were $R_{wp} = 5.41\%$, $R_p = 4.13\%$, $S = 1.94$, $R_I = 2.74\%$ and $R_F = 1.84\%$ (Table 1). The unit-cell parameters obtained for α-$(Ca_{0.85}Ba_{0.15})_3(PO_4)_2$ were $a = 13.0965(2)$, $b = 27.9046(3)$, $c = 15.4021(3)$ Å, $\alpha = \gamma = 90°$, and $\beta = 127.1224(9)°$, which are larger than those for undoped α-TCP, α-$Ca_3(PO_4)_2$. The larger cell parameters are attributable to the larger-sized Ba atoms as compared with the Ca atoms. Ionic radius of the Ba^{2+} cation for a coordination number of 7 (1.38 Å)[32] is larger than that of the Ca^{2+} cation (1.06 Å).[32] The present unit-cell parameters for Ba-substituted α-TCP were more precise and the estimated standard deviations (±0.0002 Å and ± 0.0007° to 0.0010°) in this study were much smaller than those for undoped and Si-substituted α-TCP in the literature (±0.002 to ± 0.009 Å and ± 0.02° to ± 0.1°).[12,13,15,23,24] The precise unit-cell parameters in the present study are attributable to the higher angular resolution of the diffractometer. Similarly we reported precise unit-cell parameters for undoped α-TCP by the high-resolution synchrotron powder diffractometry (±0.00012 Å and ± 0.0004°).[14]

(32) Shannon, R. D. *Acta Crystallogr.* **1976**, *32*, 751−767.

Figure 4 shows the unit-cell parameters as functions of Ba content x in $(Ca_{1-x}Ba_x)_3(PO_4)_2$. The a, b, c parameters and β angle increase with increasing Ba content. As shown in Figure 5, the unit-cell volume also increases with increasing Ba content, which is attributable to the substitution of Ca atoms by the larger-sized Ba atoms. An anisotropy in the expansion of the cell parameters by Ba doping was found for $(Ca_{1-x}Ba_x)_3(PO_4)_2$ (Figure 6). The normalized b parameter, $b(x)/b(0)$, is larger than the normalized c parameter, $c(x)/c(0)$: $b(x)/b(0) > c(x)/c(0)$. Here, $b(x)$ and $c(0)$ are the parameters b and c for $(Ca_{1-x}Ba_x)_3(PO_4)_2$ and $Ca_3(PO_4)_2$, respectively.

It is known that undoped α-TCP has a "looser" structure than undoped β-TCP.[1,14] That is presumably why α-TCP has a higher reactivity in water than β-TCP.[8] For all compositions ($x = 0.05$, 0.10, and 0.15), the unit-cell volumes of Ba-α-TCP are larger than that of undoped α-TCP, as shown in Figure 5. This suggests that the reactivity of Ba-α-TCP in water is higher than undoped α- and β-TCPs.

Figure 7 shows the crystal structure of Ba-substituted α-TCP, $(Ca_{0.85}Ba_{0.15})_3(PO_4)_2$, depicted with the refined crystallographic parameters. $(Ca_{0.85}Ba_{0.15})_3(PO_4)_2$ crystallizes in the monoclinic $P2_1/a$ with unit-cell parameters $a =$

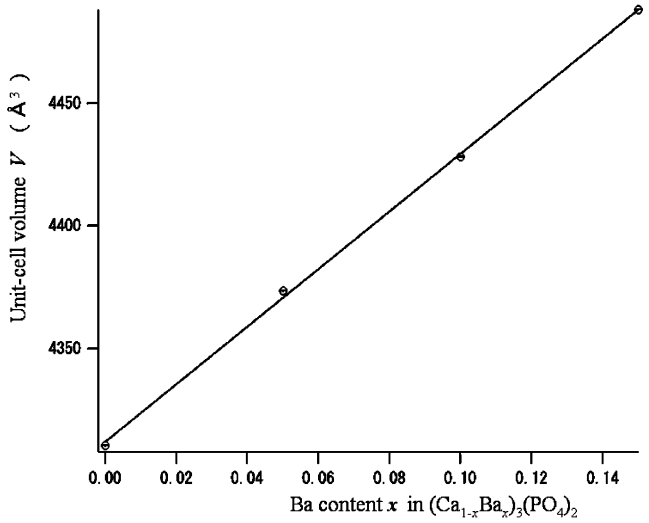

Figure 5. Unit-cell volume of the Ba-substituted α-TCP as a function of Ba content x in $(Ca_{1-x}Ba_x)_3(PO_4)_2$. Data for $x = 0$ is taken from our previous high-resolution synchrotron diffraction work.[14] Error bars of standard uncertainties in the Rietveld analysis are smaller than the datum symbols.

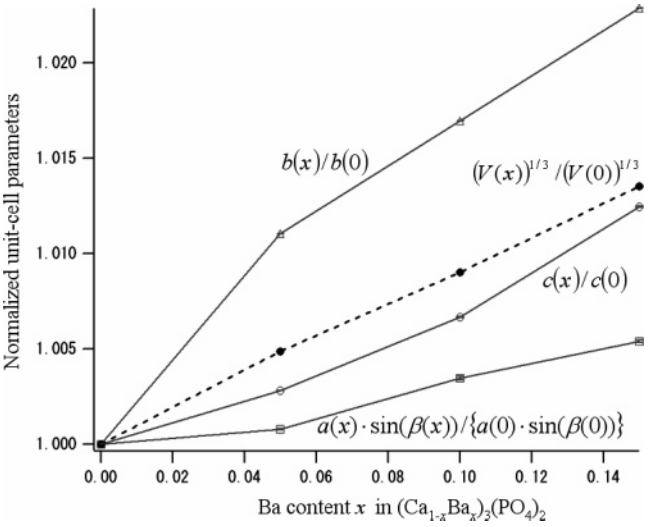

Figure 6. Normalized cell parameters as a function of Ba content, x, in $(Ca_{1-x}Ba_x)_3(PO_4)_2$. Open square: $a(x)\cdot\sin(\beta(x))/\{a(0)\cdot\sin(\beta(0))\}$; open triangles: $b(x)/b(0)$; open circles: $c(x)/c(0)$; filled circles are normalized cube root of unit-cell volume: $(V(x))^{1/3}/(V(0))^{1/3}$. Here, $a(x)$ and $V(0)$ are the unit-cell parameter a of $(Ca_{1-x}Ba_x)_3(PO_4)_2$ and unit-cell volume of undoped $Ca_3(PO_4)_2$ ($x = 0$), respectively. Error bars calculated from the standard uncertainties in the Rietveld analysis are smaller than the datum symbols.

13.0965(2), $b = 27.9046(2)$, $c = 15.4021(3)$ Å, $\alpha = \gamma = 90°$ and $\beta = 127.1224(9)°$, with 24 formula units per unit cell. The structure comprises columns of Ca^{2+} and PO_4^{3-} ions parallel to the c-axis, as shown in Figure 8. There exist cation−cation columns, ...M M M M..., and cation−anion columns, ...PO_4 M PO_4 Va PO_4 M PO_4..., where M and Va are a cation (Ca or Ba) and vacancy, respectively. These columns are arranged to form a pseudo-hexagonal pattern, as shown by the black dotted lines in Figure 8. Each cation−cation column is surrounded by six cation−anion columns. The crystal structure of Ba-substituted α-TCP is related to that of apatite. The section of the Ba-α-TCP structure that corresponds to a conventional unit cell of apatite is marked with the dashed-dotted line in Figure 8. Thus, the apatite

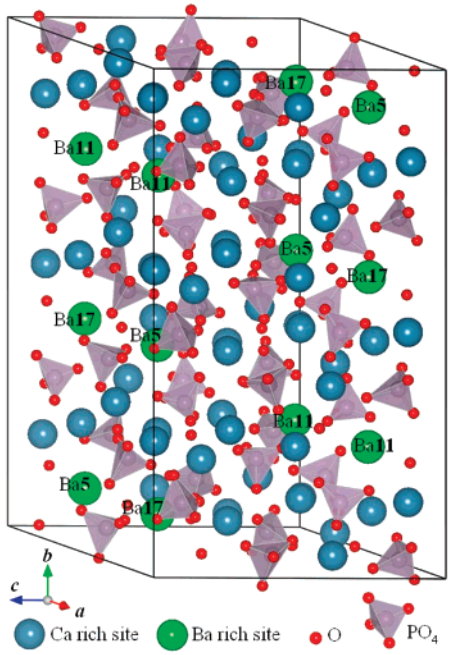

Figure 7. Crystal structure of Ba-substituted α-TCP, $(Ca_{0.85}Ba_{0.15})_3(PO_4)_2$, depicted with the refined crystallographic parameters. Solid lines denote the unit cell.

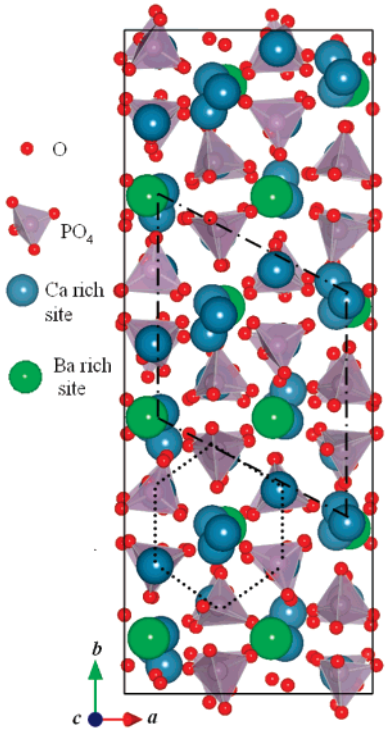

Figure 8. Crystal structure of Ba-substituted α-TCP, $(Ca_{0.85}Ba_{0.15})_3(PO_4)_2$, depicted with the refined crystallographic parameters. The dotted and dotted-dashed lines are the pseudo-hexagonal channel and conventional apatite cell, respectively. Solid lines denote the unit cell.

can be derived from Ba-α-TCP by replacing the cation−cation columns at the corners of the apatite cell by cation−anion columns. These structural features of Ba-substituted α-TCP were also reported for the undoped α-TCP.[1,12]

As shown in Figures 7 and 8, the Ba atoms are substituted for the Ca sites. Figure 9 shows the variation of occupancy factors of Ba atoms at the ith cation sites g(Bai) in the Ba-substituted α-TCP with Ba content x in $(Ca_{1-x}Ba_x)_3(PO_4)_2$. Most of the Ba atoms are located at three crystallographic

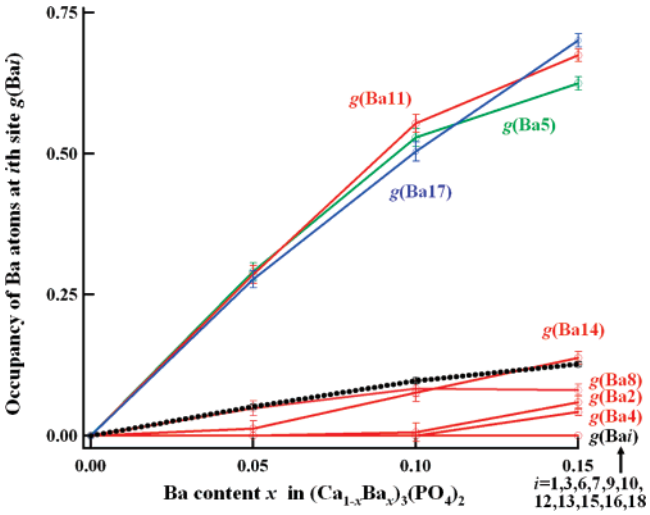

Figure 9. Variation of occupancy factor of Ba atoms at the *i*th cation sites *g*(Ba*i*) in the Ba-substituted α-TCP with Ba content, *x*, in $(Ca_{1-x}Ba_x)_3(PO_4)_2$.

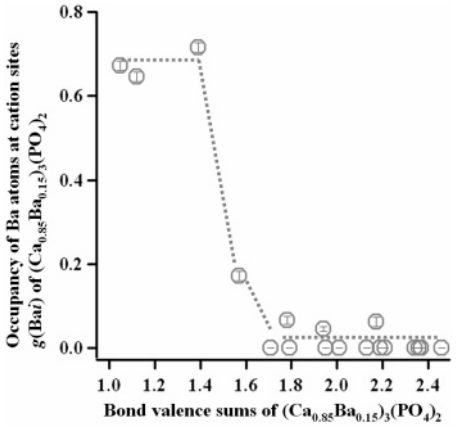

Figure 10. Relationship between the bond valence sum and occupancy factor of Ba atoms at eighteen cation sites in α-$(Ca_{0.85}Ba_{0.15})_3(PO_4)_2$. The dotted lines are guides for the eye.

sites of Ca17, Ca11, and Ca5 among the eighteen cation sitesin the α-$(Ca_{1-x}Ba_x)_3(PO_4)_2$(x = 0.05, 0.10, and 0.15). The refined positional parameters and occupancy factors of the preferred sites for Ba substitutions were Ca17: (0.0909(6), 0.4167(2), 0.7823(5)) g(Ba) = 0.72(2); Ca11: (0.4068(6), 0.2506(2), 0.2199(5)) g(Ba) = 0.67(1); Ca5: (0.0983(6), 0.0837(2), 0.7857(5)) g(Ba) = 0.65(1) in the α-$(Ca_{0.85}Ba_{0.15})_3(PO_4)_2$. The occupancy factors of Ba atoms at these sites increase with Ba content. Small fractions of Ba atoms are also located at the Ca2, Ca4, Ca8, and Ca14 sites. In some preliminary analyses, the occupancy factors of Ba atoms at the other Ca*i* sites (i = 1, 3, 6, 7, 9, 10, 12, 13, 15, 16, 18) were refined to be zero within the estimated standard deviations; thus, we fixed these values to zero in the final refinement. The bond valence sums (BVS)[33] were calculated for all the cation sites in $(Ca_{1-x}Ba_x)_3(PO_4)_2$ (x = 0.15 and 0.00) to validate the present results of the occupancies (Table 2 and Figure 10). Bond valence parameter for the cation was assumed to be 1.967, which is the value for the Ca^{2+} cation in oxides.[33] The occupancy factor decreases with increasing BVS value (Figure 10). The BVS of the Ba-rich sites, namely, Ca5, Ca11, and Ca17, have smaller values, as shown in Table 2. This indicates the Ba atoms prefer the crystallographic sites with smaller BVS values and weaker bonding. These results are consistent with the refined occupancies: Most of the Ba atoms are located at the Ca5, Ca11, and Ca17 sites. Table 2 lists the coordination number (CN), average bond length, BVS, polyhedral volume, and distortion indices[34] for $(Ca,Ba)O_{CN}$ polyhedron. Comparing with the CN, bond length, polyhedral volume, and distortion indices, the BVS exhibits clear correlation with the refined occupancy factors of Ba atoms.

Table 2. Coordination Number CN, Occupancy Factor of Ba Atoms *g*(Ba), Average Bond Length <*r*>, Bond Valence Sum BVS, Volume of Polyhedron, and Distortion Indices[34] for the $(Ca,Ba)O_{CN}$ Polyhedron of Undoped and Ba-Substituted α-TCP, $(Ca_{1-x}Ba_x)_3(PO_4)_2$ (x = 0.00 and 0.15)

composition x	site	CN	g(Ba)	<r> (Å)	BVS	volume of polyhedron (Å^3)	distortion index
0	Ca1	7	0	2.46	1.94	20.0	0.035
0.15	Ca1	8	0	2.55	1.79	26.5	0.052
0	Ca2	7	0	2.46	1.95	20.9	0.044
0.15	Ca2	7	0.062(11)	2.53	2.17	17.9	0.106
0	Ca3	7	0	2.44	2.09	20.8	0.042
0.15	Ca3	7	0	2.47	2.34	20.7	0.094
0	Ca4	6	0	2.35	2.16	16.2	0.018
0.15	Ca4	6	0.046(6)	2.40	1.94	16.9	0.040
0	Ca5	7	0	2.52	1.62	19.9	0.033
0.15	Ca5	7	0.646(11)	2.68	1.12	24.9	0.042
0	Ca6	7	0	2.45	2.04	20.1	0.046
0.15	Ca6	7	0	2.47	2.13	22.0	0.052
0	Ca7	8	0	2.53	2.00	26.3	0.064
0.15	Ca7	8	0	2.52	2.19	25.5	0.080
0	Ca8	7	0	2.48	1.86	19.9	0.042
0.15	Ca8	7	0.066(10)	2.56	1.78	21.2	0.085
0	Ca9	6	0	2.37	2.03	15.5	0.025
0.15	Ca9	7	0	2.42	2.37	19.3	0.066
0	Ca10	6	0	2.34	2.21	15.4	0.028
0.15	Ca10	6	0	2.32	2.36	15.2	0.016
0	Ca11	6	0	2.441	1.87	14.4	0.064
0.15	Ca11	7	0.672(11)	2.77	1.05	31.3	0.059
0	Ca12	7	0	2.454	1.96	21.2	0.036
0.15	Ca12	10	0	2.63	1.71	33.3	0.069
0	Ca13	7	0	2.440	2.05	20.11	0.042
0.15	Ca13	7	0	2.4831	1.95	20.8	0.053
0	Ca14	7	0	2.516	1.80	17.2	0.066
0.15	Ca14	6	0.172(11)	2.52	1.57	14.4	0.082
0	Ca15	7	0	2.393	2.26	19.3	0.023
0.15	Ca15	7	0	2.4023	2.46	19.2	0.068
0	Ca16	6	0	2.340	2.22	16.1	0.020
0.15	Ca16	6	0	2.35	2.21	16.1	0.039
0	Ca17	7	0	2.512	1.85	20.0	0.075
0.15	Ca17	5	0.716(11)	2.51	1.39	12.6	0.082
0	Ca18	7	0	2.424	2.07	21.0	0.021
0.15	Ca18	8	0	2.45	2.01	19.2	0.037

These values were calculated for the $(Ca,Ba)O_{CN}$ polyhedron consisting of a cation and anions with the cation−anion bonds less than 3 Å. Calculations for x = 0.15 and 0.00 were performed using the crystallographic parameters of the present refinement and in the literature,[12] respectively.

Figure 11 shows the relationship between the occupancy factor of Ba atoms in α-$(Ca_{0.85}Ba_{0.15})_3(PO_4)_2$ and BVS in undoped α-$Ca_3(PO_4)_2$. The bond valence sums of the Ba-rich sites, Ca5, Ca11, and Ca17, have smaller values even for undoped α-$Ca_3(PO_4)_2$, as shown in Figure 11. The undoped α-TCP has a variety of coordination environments at the Ca sites. This suggests that the BVS values in undoped α-TCP are indications of the preference of the occupation of dopant cations. The Ba cation has relatively large ionic

(33) Brese, N. E.; O'Keeffe, M. *Acta Crystallogr. B* **1991**, *47*, 192−197.

(34) Robinson, K.; Gibbs, G. V.; Ribbe, P. H. *Science* **1971**, *172*, 567−570.

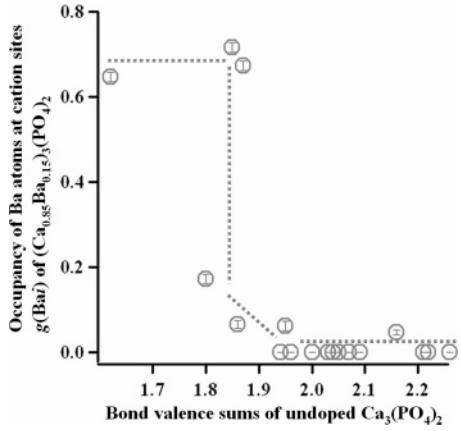

Figure 11. Relationship between the occupancy factor of Ba atoms in α-$(Ca_{0.85}Ba_{0.15})_3(PO_4)_2$ and bond valence sums in undoped α-$Ca_3(PO_4)_2$. The dotted lines are guides for the eye.

radius, leading to the preference of sites with smaller BVS values, while small cations such as Mg^{2+} might preferentially occupy crystallographic sites with larger BVS values (e.g., Ca10, Ca15, and Ca16 sites).

Concluding Remarks

In the present study, Ba-α-TCPs, $(Ca_{1-x}Ba_x)_3(PO_4)_2$ (x = 0.05, 0.10, and 0.15), have been prepared by solid-state reactions. Crystal structure of the Ba-α-TCP powders has been investigated by high-resolution synchrotron powder diffraction and the Rietveld method. Diffraction data were successfully analyzed by the single-phase Ba-α-TCP (space group $P2_1/a$). Unit cell parameters a, b, c, and β increase with increasing Ba content. The unit-cell volume also increases with Ba content, which is ascribed to the substitution of Ca atoms by the larger-sized Ba atoms. The large cell volumes of the Ba-α-TCPs suggest that they would exhibit a high reactivity in water. Most of the Ba atoms are located at three crystallographic sites, namely Ca17: (0.0909, 0.4167, 0.7823) g(Ba17) = 0.72(2); Ca11: (0.4068, 0.2506, 0.2199) g(Ba11) = 0.67(1); Ca5: (0.0983, 0.0837, 0.7857) g(Ba5) = 0.65(1) among the eighteen cation sites in the α-$(Ca_{1-x}Ba_x)_3(PO_4)_2$(x = 0.05, 0.10, and 0.15). These sites have relatively smaller BVS, indicating the preference sites for the larger-sized Ba substitutions. The BVS values for the cation sites in undoped α-TCP would be indications of the occupation of dopant cations.

Acknowledgment. We express special thanks to Dr. T. Ikeda for useful suggestions on the Rietveld analysis. We thank to Mr. T. Wakita and Daiichi Kigenso Kagaku Co. for the chemical analysis. This research was supported in part by the Ministry of Education, Culture, Sports, Science and Technology of Japan through a Grant-in-Aid for Scientific Research (B) and by the Inamori Foundation. Figures 7 and 8 were prepared using the VENUS and VESTA programs developed by Dr. R. Dilanian, Dr. F. Izumi, and Mr. K. Momma.

Supporting Information Available: Crystallographic information data in CIF format. This material is available free of charge via the Internet at http://pubs.acs.org.

CM070963Y